Pharmaceutical Research, Vol. 26, No. 7, July 2009 (© 2009)
DOI: 10.1007/s11095-009-9882-6

Research Paper

Diffusion Studies of Nanometer Polymersomes Across Tissue Engineered Human Oral Mucosa

Vanessa Hearnden,[1,2] Hannah Lomas,[1] Sheila MacNeil,[1] Martin Thornhill,[2] Craig Murdoch,[2] Andrew Lewis,[3] Jeppe Madsen,[4] Adam Blanazs,[4] Steve Armes,[4] and Giuseppe Battaglia[1,5]

Received August 15, 2008; accepted March 19, 2009; published online April 22, 2009

Purpose. To measure the diffusion of nanometer polymersomes through tissue engineered human oral mucosa.
Methods. *In vitro* models of full thickness tissue engineered oral mucosa (TEOM) were used to assess the penetration properties of two chemically different polymersomes comprising two of block copolymers, PMPC-PDPA and PEO-PDPA. These copolymers self-assemble into membrane-enclosed vesicular structures. Polymersomes were conjugated with fluorescent rhodamine in order to track polymersome diffusion. Imaging and quantification of the diffusion properties were assessed by confocal laser scanning microscopy (CLSM).
Results. TEOM is morphologically similar to natural oral mucosa. Using CLSM, both formulations were detectable in the TEOM within 6 h and after 48 h both penetrated up to 80 μm into the TEOM. Diffusion of PMPC-PDPA polymersomes was widespread across the epithelium with intra-epithelial uptake, while PEO-PDPA polymersomes also diffused into the epithelium.
Conclusions. CLSM was found to be an effective and versatile method for analysing the level of diffusion of polymersomes into TEOM. The penetration and retention of PMPC-PDPA and PEO-PDPA polymersomes means they may have potential for intra-epithelial drug delivery and/or trans-epithelial delivery of therapeutic agents.

KEY WORDS: confocal laser scanning microscopy; diffusion; epithelium; oral mucosa; polymersome.

INTRODUCTION

Historically, most *in vitro* biological research has relied on two-dimensional monolayer cell culture studies. Whilst these can provide valuable information regarding cell behaviour and responses, they are poor at replicating the three-dimensional behaviour of tissues and are not always clinically relevant or representative of the *in vivo* situation. Furthermore, because of differences in the cell microenvironment, cells grown in three-dimensional tissue engineered models behave differently than those cultured as monolayers (reviewed in (1,2)). Three-dimensional tissue engineered models of human tissue that accurately reflect the *in vivo* situation are a very valuable tool for studies of toxicity and diffusion (3,4). In this study we used a full thickness tissue engineered *in vitro* model of the oral mucosa. These models comprise de-epidermised acellular human dermis repopulated with laboratory-expanded primary human oral epithelial cells and fibroblasts (5). Selvaratnam *et al.* have compared the permeability of a TEOM, similar to the one used here, with normal human buccal mucosa from adult necropsies (6) and found that the permeability constant, as assessed using permeation of tritated water, was very similar in the model and intact oral mucosa. The TEOM used in this study has been developed for clinical applications (7) and has been used successfully in the clinic to replace scarred tissue in the urethra with nearly 3 years follow-up (8), confirming the physiological relevance of this tissue.

Polymersomes are macromolecular aggregates formed in aqueous solution from amphiphilic block copolymers. Their design is based on a concept found in many biological systems, most clearly in cell membranes. Amphiphilic molecules containing a hydrophobic portion and a hydrophilic portion self-assemble when in contact with water to achieve the most entropically favourable configuration. The configuration of the structure depends on the concentration of the molecules and the hydrophilic/hydrophobic balance (9,10,12,13). In this study

[1] Biomaterials and Tissue Engineering Group, Department of Engineering Materials, Kroto Research Institute, North Campus, University of Sheffield, Broad Lane, Sheffield, S3 7HQ, UK.
[2] Department of Oral & Maxillofacial Medicine & Surgery, School of Clinical Dentistry, University of Sheffield, Sheffield, UK.
[3] Biocompatibles UK Ltd., Farnham, Surrey, UK.
[4] Department of Chemistry, University of Sheffield, Brook Hill, Sheffield, S3 7HF, UK.
[5] To whom correspondence should be addressed. (e-mail: g.battaglia@sheffield.ac.uk)

ABBREVIATIONS: ALI, Air liquid interface; ATRP, Atomic transfer radical polymerisation; CLSM, Confocal laser scanning microscopy; DED, De-epithelialized dermis; PEO_{23}-$PDPA_{15}$, Poly(ethylene oxide)-poly(2-(diisopropylamino)ethyl methacrylate); $PMPC_{25}$-$PDPA_{70}$, 2-(Methacryloyloxy)ethyl phosphorylcholine)-poly(2-(diisopropylamino) ethyl methacrylate; THF, Tetrahydrofuran; TEM, Transmission electron microscopy; TEOM, Tissue engineered oral mucosa.

we used membrane-enclosed spherical vesicular structures, known as polymersomes.

The first membrane-enclosed structures designed in a laboratory were liposomes made from naturally-derived phospholipids (14). Liposomes have now been developed for use as drug carriers for hydrophobic drugs as well as carriers of DNA for transfection (15). Unfortunately, although liposomes are fairly biocompatible they exhibit low circulation times in the bloodstream and have poor stability (16). To increase circulation times, stealth liposomes coated with poly(ethylene glycol) (PEG) were developed to reduce detection from the body (17). However, the release profile of materials encapsulated into these liposomes is hard to control; some material leaks out quickly while other material never gets released (18–20). Moreover, relying on naturally occurring phospholipids restricts opportunities to adapt liposome properties into more efficient delivery vehicles. The difficulties experienced with liposomes led to the generation of polymersomes; polymer vesicles created *via* the self-assembly of amphiphilic block copolymers (12). By making these membrane-enclosed structures from synthetic amphiphiles the stability of the structure is improved and their properties can be tailored to meet their desired application (13). In addition, polymersomes comprise relatively high molecular weight polymer chains compared to phospholipids and these show a high level of entanglement within the bilayer membrane, improving stability compared to liposomes (21). Polymersome membranes can also be ten times less permeable to water than phospholipid bilayers making them far less leaky and more retentive as drug delivery vectors than liposomes (12,22). Both liposomal bilayer membranes and polymersome membranes have the ability to remodel and heal if damaged due to the hydrophobic effect (23).

Polymersomes are capable of encapsulating both hydrophobic molecules, such as many cancer drugs, and hydrophilic molecules such as DNA and proteins. Materials thus far encapsulated into polymersomes include DNA for transfection (24,25), anticancer drugs for intracellular delivery (20), haemoglobin for blood substitutes (26,27) and contrast agents for *in vivo* imaging (28). Antibodies have also been conjugated to polymersomes for targeted delivery (29).

Major advances in polymer chemistry have opened up many possibilities for block copolymer formulations and therefore numerous polymersome structures (30). The degradation of polymersomes can be adjusted using different polymer formulations. pH sensitive polymersomes (10), oxidative species (31) and biodegradable polymers all degrade within the body in response to different stimuli (26,32,33).

Delivery of drugs into or across the oral mucosa is difficult because of the relative impermeability of the oral epithelium. Delivery of drugs into the epithelium (intra-epithelial delivery), is important for the treatment of many mucosal diseases such as squamous cell carcinoma (34). Alternatively, trans-mucosal drug delivery offers the possibility to deliver drugs quickly and effectively into the circulation without the need for injection and avoiding the first-pass metabolism of orally-delivered treatments. Trans-epithelial delivery has been the focus of much research (35). Polymersomes have the potential to provide a delivery system which is able to deliver intra-epithelial and trans-epithelial therapies. To achieve an effective delivery system it is essential to have a reproducible *in vitro* test system that allows us to study and track polymersome penetration and retention within the different compartments of the oral mucosa.

Here, using confocal laser scanning microscopy, we investigate the diffusion properties of polymersomes synthesised from two block copolymers (2-(methacryloyloxy)ethyl phosphorylcholine)-poly(2-(diisopropylamino)ethyl methacrylate) ($PMPC_{25}$-$PDPA_{70}$) and poly(ethylene oxide)-poly(2-(diisopropylamino)ethyl methacrylate) (PEO_{23}-$PDPA_{15}$) across TEOM, with long-term view of developing a targeted intra- and trans-epithelial drug delivery systems. To the best of our knowledge, this is the first study to examine penetration of nanomaterials through a tissue engineered epithelia.

MATERIALS AND METHODS

2-(Methacryloyloxy)ethyl phosphorylcholine (MPC; >99%) was provided by Biocompatibles UK Ltd. 2-(Diisopropylamino)ethyl methacrylate (DPA; Scientific Polymer Products, USA) was passed through the column supplied by the manufacturer to remove inhibitor. Copper(I) bromide (CuBr; 99.999%), copper(I) chloride (CuCl; 99.995%), 2,2′-bipyridine (bpy, 99%), 2-bromoisobutyl bromide, triethylamine, methanol, tetrahydrofuran (THF) and isopropanol were purchased from Sigma-Aldrich UK (Poole, Dorset, UK) and were used as received. Column chromatography grade silica gel 60 (0.063–0.200 mm) used for removal of the atom transfer radical polymerisation (ATRP) copper catalyst was purchased from E. Merck (Darmstadt, Germany). Monohydroxy-capped poly(ethylene oxide) was purchased from Fluka (Poole, Dorset, UK) and freeze-dried before use to remove water. Regenerated Cellulose (RC) dialysis tubing (Spectra Por® 6, molecular weight cut-off 3.5 kDa) was purchased from Spectrum Labs (Rancho Dominguez, CA, USA). 2-(N-Morpholino)ethyl 2-bromo-2-methylpropanoate (ME-Br) initiator and poly(ethylene oxide) macro-initiator (PEO-Br) were synthesized according to a previously reported procedure (36).

$PMPC_{25}$-$PDPA_{70}$ Copolymer Synthesis

$PMPC_{25}$-$PDPA_{70}$ copolymer was synthesized by ATRP as reported elsewhere (Fig. 1a) (10). Briefly, a Schlenk flask with a magnetic stir bar and a rubber septum was charged with CuBr (25.6 mg, 0.178 mmol) and MPC (1.32 g, 4.46 mmol). ME-Br initiator (50.0 mg, 0.178 mmol) and bpy ligand (55.8 mg, 0.358 mmol) were dissolved in methanol (2 ml), and this solution was deoxygenated by bubbling N_2 for 30 min before being injected into the flask using a syringe. The [MPC]:[ME-Br]:[CuBr]:[bpy] relative molar ratios were 25:1:1:2. The polymerization was conducted under a nitrogen atmosphere at 20°C. After 65 min, a mixture of deoxygenated DPA (2.67 g, 12.5 mmol) and methanol (3 ml) was injected into the flask. After 48 h, the reaction solution was diluted by addition of 200 ml isopropanol and then passed through a silica column to remove the spent Cu catalyst.

Rhodamine (Rho)-PMPC$_{30}$PDPA$_{60}$ Copolymer Synthesis

Rho-PMPC$_{30}$-PDPA$_{60}$ copolymer was synthesized by an ATRP procedure as reported previously (Fig. 1b) (11). Briefly, a Schlenk flask with a magnetic stir bar and a rubber septum was charged with MPC (1.20 g, 4.05 mmol). A rhodamine 6G-based initiator (Rho initiator), prepared in-house (83.8 mg, 0.135 mmol) was dissolved in anhydrous methanol (0.75 ml) and added to the MPC (manuscript in preparation). The flask was washed with 0.75 ml anhydrous methanol which was added to the MPC solution. The solution was then deoxygenated by bubbling N_2 for 30 min. After this period, a mixture of CuBr (19.37 mg, 0.135 mmol) and bpy ligand (42.17 mg, 0.171 mmol) was added to the reaction mixture after mixing the solids with a spatula. The [MPC]:[Rho]:[CuBr]:[bpy] relative molar ratios were 30:1:1:2. The reaction was carried out under a N_2 atmosphere at 20°C. After 40 min, deoxygenated DPA (1.73 g, 8.10 mmol) and methanol (2 ml) mixture was injected into the flask. After 48 h, the reaction solution was diluted by addition of methanol (about 70 ml) and opened to the atmosphere. When the resulting suspension had turned green, 200 ml chloroform was added to thoroughly dissolve the copolymer and the resulting solution was passed through a silica column to remove the catalyst. After removal of the solvent, the solid was taken up into 3:1 chloroform:methanol and dialyzed for 3 days against this solvent mixture with daily changes of solvent to remove residual bpy ligand. After evaporation, the solid was dispersed in water, freeze-dried and dried in a vacuum oven at 80°C for 48 h.

PEO$_{23}$-PDPA$_{15}$ Copolymer Synthesis (Fig. 1c)

DPA monomer, PEO$_{23}$-Br macro-initiator and bpy were weighed into a round-bottomed flask. Methanol was separately degassed under N_2 for 20 min, added to the reaction solution (overall monomer concentration=50% *v*/*v*) and further degassed for 10 min. This mixture was then heated to 50°C and CuCl catalyst added under constant nitrogen flow to allow the reaction solution to turn dark brown and become more viscous, indicating the onset of polymerization. After polymerization for 16 h, an aliquot was removed for ^{1}H NMR analysis. The reaction was terminated by exposure to air after ^{1}H NMR indicated no remaining monomer (>99.9% conversion). The crude copolymer was dissolved in THF and the spent catalyst removed by column chromatography (silica stationary phase). Evaporation of the THF produced a viscous yellow copolymer. To remove un-reacted initiator and bpy from reaction product, the copolymer was dissolved in the minimal amount of THF and dialyzed against water for 7 days followed by dialysis against methanol for 2 days. After evaporation, a colorless viscous copolymer was obtained which was dried under vacuum and characterized by ^{1}H NMR and THF gel permeation chromatography (GPC).

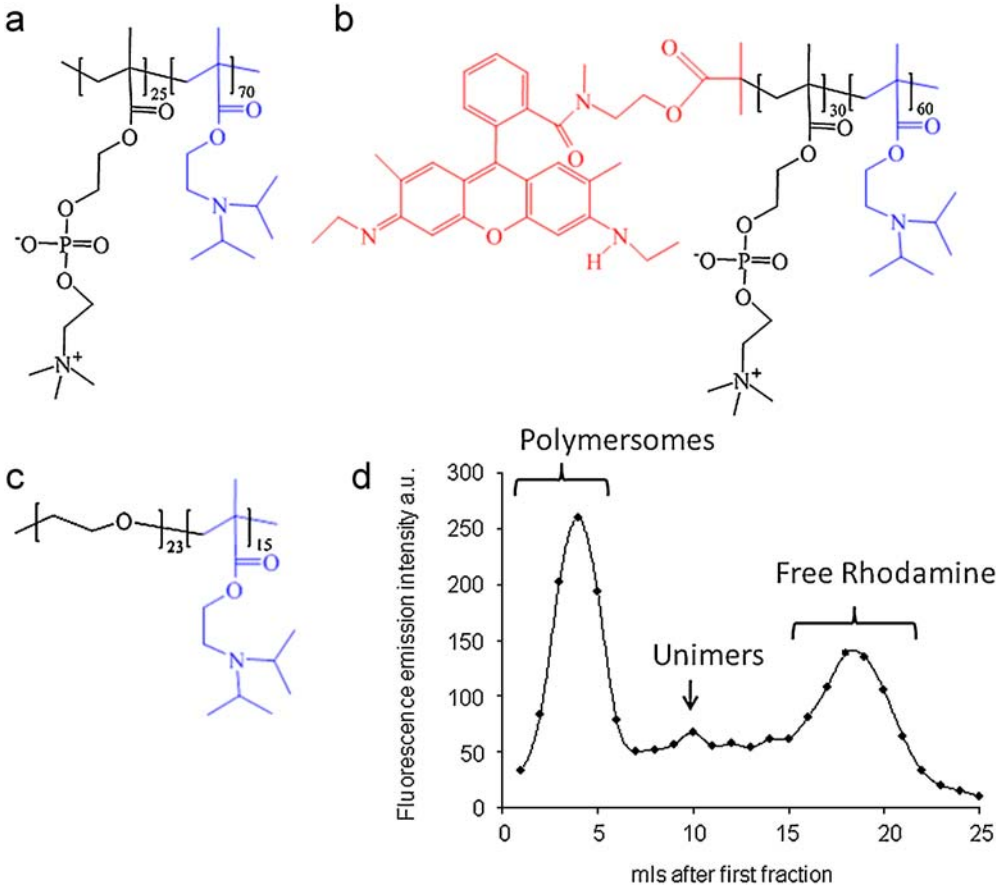

Fig. 1. Chemical structures of PMPC$_{25}$-PDPA$_{70}$ (**a**), Rho-PMPC$_{30}$-PDPA$_{60}$ (**b**) and PEO$_{23}$-PDPA$_{15}$ (**c**). Fluorescence emission of fractions collected from GPC column (**d**), excitation 540 nm, emission 560 nm.

Production of Polymersomes

$PMPC_{25}$-$PDPA_{70}$ or PEO_{23}-$PDPA_{15}$ (890 nM) were dissolved in a glass vial in 2:1 chloroform:methanol solution. For rhodamine-labelled samples, 5% (*v*/*v*) dissolved rhodamine-labelled polymer (Rho-$PMPC_{30}PDPA_{60}$) was added to the polymer solution. A copolymer film was formed by evaporating the solvent overnight in a vacuum oven at 50° C. The film was then rehydrated using 2 ml pH 2 PBS (100 mM). Once the film dissolved the pH was increased to 7.4. This solution was sonicated for 5 min (Sonicor Instruments Corporation, NY, USA) and then purified by gel permeation chromatography using a sepharose 4B size exclusion column to extract the fraction containing vesicles and remove any remaining free rhodamine dye.

Removal of Free Rhodamine

One ml fractions from the GPC column were collected, diluted 1 in 10 with PBS and the fluorescence of 1 ml of this solution measured using a fluorescence spectrophotometer with excitation set at 540 nm and emission at 560 nm (Varian Cary Eclipse, CA, USA). Polymersomes were contained in fractions 2 ml to 5 ml (Fig. 1d). The subsequent fractions (>5 ml) contained unimers and free rhodamine and were discarded.

Transmission Electron Microscopy (TEM) Analysis of Polymersomes

For TEM analysis, samples were mounted onto pre-carbon-coated copper grids. Grids were first glow discharged for 40 s, and then submerged into the polymersome solution (10 mg/ml for both polymersome solutions) for 60 s. The grids were then blotted dry and submerged into a phosphotungstic acid solution (0.75% *w*/*v*, made up using distilled water) for 20 s, before being blotted dry and briefly dried under vacuum. Imaging was performed on a Philips CM100 instrument operating at 80 kV equipped with a Gatan 1 k CCD camera.

Cell Culture

Normal oral keratinocytes (NOK) and fibroblasts (NOF) were isolated from oral mucosal biopsies obtained from consenting patients during oral surgical procedures. The biopsies were incubated overnight at 4°C in 0.1% *w*/*v* Difco trypsin solution supplemented with 100 IU/ml penicillin, 100 mg/ml streptomycin and 0.625 μg/ml amphotericin B. The epithelium was then peeled from the connective tissue component. Keratinocytes were gently scraped from the underside of the epithelium and the top side of the connective tissue layer using a scalpel. Keratinocytes were cultured according to the method of Rheinwald and Green (37). Briefly, cells were cultured on an irradiated mouse fibroblast (i3T3) feeder layer in Green's media composed of Dulbecco's modified Eagle's medium (DMEM) and Hams F12 medium in a 3:1 (*v*/*v*) ratio, supplemented with 10% (*v*/*v*) foetal calf serum (FCS), 100 IU/ml penicillin, 100 mg/ml streptomycin and 0.625 μg/ml amphotericin B, 0.1 μM cholera toxin, 10 ng/ml epidermal growth factor (EGF), 0.4 μg/ml hydrocortisone, 0.18 mM adenine, 5 μg/ml insulin, 5 μg/ml transferrin, 2 mM glutamine and 0.2 μM triiodothyronine. The media used to culture the NOK was removed and replenished every 3–4 days until the culture flasks were 80% confluent. To passage the cells i3T3 cells were detached using 0.02% EDTA solution for 5 min before removal of NOK from the flasks using trypsin/0.02% EDTA solution.

NOF were isolated from the connective tissue of oral biopsies. The connective tissue was finely minced and incubated at 37°C in a 5% CO_2 humidified incubator overnight in 10 ml of 0.5% collagenase A. The isolated fibroblasts were cultured in DMEM supplemented with 10% (*v*/*v*) FCS, 100 IU/ml penicillin, 100 mg/ml streptomycin and 0.625 μg/ml amphotericin B. Keratinocytes were used up to passage 3 and fibroblasts between passage 3 and 8.

Preparation of Sterilized De-Epithelized Dermis (DED)

Skin obtained from consenting donors was stored at 4°C in DMEM supplemented with 10% (*v*/*v*) FCS, 100 IU/ml penicillin, 100 mg/ml streptomycin and 0.625 μg/ml amphotericin B for 7 days. DED was de-cellularized in 1 M sodium chloride for at least 8 h. This method removes the epidermis but retains basement membrane proteins such as collagen IV and laminin, which aids the subsequent attachment of NOKs in the 3D culture.

Culture of 3D Tissue Engineered Oral Mucosa

TEOM was generated using a previously established method (7) with the exception that the DED was not sterilised for these *in vitro* studies. DED was cut into 2 cm× 2 cm squares and placed into six well plates submerged in Green's media. Chamfered surgical stainless steel rings with an internal diameter of 6 mm were pushed onto the DED to provide a liquid tight seal. One milliliter of cell suspension containing 5×10^5 NOKs and 2.5×10^5 NOFs in Green's media was added into the ring. Green's media was also added outside the ring to stop the cell solution leaking out (Fig. 2, step 1). After 2 days half the media inside the ring was removed and replenished with fresh media. On day 3 DED with cells attached was brought to an air-liquid interface (ALI) using a stainless steel grid. The underside of the model was in contact with Green's media while the top was exposed to the air to encourage epithelial stratification (Fig. 2, step 2). Models were cultured for 10–14 days at the ALI. One hundred μl of rhodamine-labelled polymersome was added to the top surface of the model in a plastic ring and incubated for up to 48 h (Fig. 2, step 3). Before imaging the models were carefully washed three times in PBS and left submerged in PBS for laser scanning confocal imaging.

Confocal Laser Scanning Microscopy (CLSM)

CLSM imaging was done with the samples submerged in PBS using an Acroplan ×40 dipping lens (Carl Zeiss, Jena, Germany) on an upright confocal microscope (Zeiss LSM 510 Meta, Jena, Germany). CLSM was used to determine the spectra of autofluorescence emitted from the TEOM and emission spectra of samples exposed to rhodamine-labelled polymersomes. Samples were excited at 488 nm or 543 nm and emission was detected every 10.45 nm. All measurements

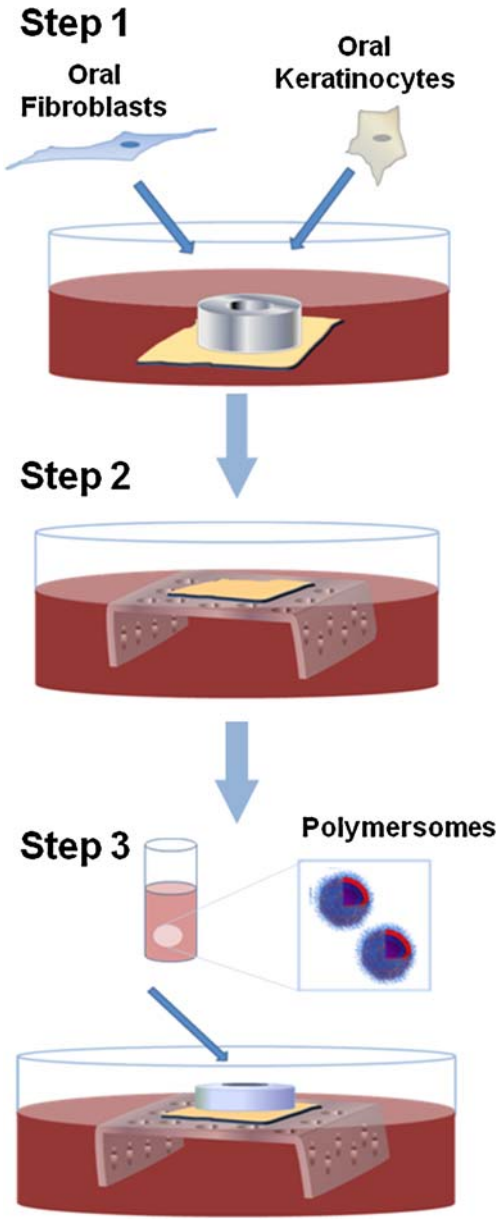

Fig. 2. Schematic diagram of the method used to culture tissue engineered full thickness oral mucosa. Primary oral keratinocytes and oral fibroblasts are seeded onto a DED scaffold (*step 1*). After cell attachment the DED is raised to an air–liquid interface to encourage epithelial stratification using a stainless steel grid (*step 2*). After culturing for 10–14 days at the air-liquid interface, polymersomes are added to the top surface of the models (*step 3*).

were taken using the same excitation intensity and detector gain. Excitation at 488 nm, emission>505 nm detects autofluorescence from the collagen and other proteins in the sample. Excitation at 543 nm detects rhodamine. As the rhodamine is covalently attached in the Rho-PMPC-PDPA polymer, this method of detection enables tracking of the polymersomes. Three dimensional images of 200 μm×200 μm×100–200 μm were obtained using the z-stack function. These images are made up of 50–100 images 2 μm apart.

Histological Analysis

For histological analysis TEOM were fixed in 3% paraformaldehyde for 24 h, processed and embedded in paraffin wax. Four micrometer sections were cut, de-waxed, stained with haematoxylin and eosin and mounted on slides for analysis.

RESULTS

Characterization of TEOM

Fig. 3 shows histological analysis of (a) a normal oral mucosa biopsy and (b) the TEOM. This is a full thickness model as it contains both a stratified epithelium and a connective tissue component containing fibroblasts. Both images show the presence of a well attached epithelial layer indicating a good epithelial/connective tissue junction, highly prolific basal epithelial cells and differentiating cells in the upper layers of the epithelium. In addition, they both have a dense fibrous connective tissue containing fibroblasts. This model is representative of normal stratified squamous oral epithelium (38).

In Fig. 4 we show the emission spectra of the oral mucosa model when excited at 488 nm and 543 nm. Both spectra were taken using the same settings and the same excitation intensity. There is a broad emission of autofluorescence from the TEOM when excited at 488 nm (Fig. 4a) but very little when excited at 543 nm (Fig. 4b). The autofluorescence comes predominantly from the extra-cellular matrix (ECM) proteins (39). To avoid autofluorescence as far as possible we used rhodamine 6G to label the polymersomes, since this group exhibits maximum fluorescence intensity at 543 nm.

Quantification and Characterization of Polymersome Penetration into Oral Mucosa

Transmission electron micrographs (TEM) show membrane-enclosed spherical structures with diameters of around 100 nm for both formulations (Fig. 5a, b).

After exposure of TEOM to rhodamine labelled polymersomes the emission spectra arising from 543 nm excitation changes dramatically, demonstrating the presence of polymersomes (Fig. 6a). Fig. 6b shows a confocal image of TEOM excited at 488 nm and 543 nm after 48 h exposure to polymersomes while Fig. 6c shows the control model without polymersome exposure. Combining both excitation channels gives a composed image. A negative control of unlabelled polymersomes also showed no fluorescence in the 543 nm channel (data not shown). Here we have tracked the diffusion of polymersomes across the oral epithelium using confocal laser scanning microscopy (CLSM).

The diffusion of both PEO_{23}-$PDPA_{15}$ and $PMPC_{25}$-$PDPA_{70}$ polymersomes into the TEOM is time-dependent. In Fig. 7 the *z*–*x* plane shows a cross section through the full thickness model. After 6 h exposure to rhodamine-labelled polymersomes synthesized from either polymer, rhodamine (red) fluorescence can be seen in the most superficial epithelial layers of the model (Fig. 7b, e). The position of the polymersomes with respect to the epithelial/connective tissue interface can be judged from the relative positions of

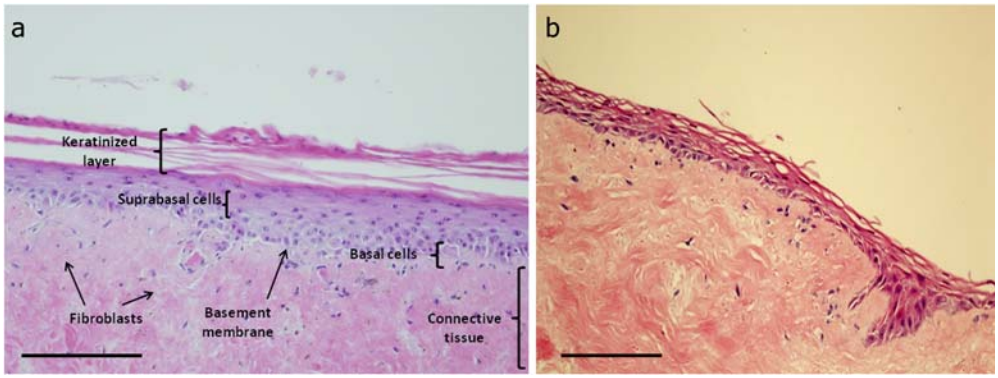

Fig. 3. Haematoxylin and eosin stained sections of an oral mucosa biopsy from a healthy patient (**a**) and TEOM cultured for 10 days at air liquid interface (**b**). *Scale bar* 200 μm.

the red fluorescence of the polymersomes and the blue autofluorescence of the connective tissue. Due to the high ECM protein content of the connective tissue, the autofluorescence of the connective tissue is more intense than from the epithelium, which appears relatively dark. Fig. 7c, f and g clearly show a layer of rhodamine fluorescence in the superficial cells of the epithelium, above a darker region (the basal layers of epithelium) which lies above the highly autofluorescent connective tissue. After 30 h there is more widespread uptake of polymersomes by the superficial epithelial cells for the $PMPC_{25}$-$PDPA_{70}$ polymersomes than the PEO_{23}-$PDPA_{15}$ (Fig. 7c, f). After 48 h exposure to $PMPC_{25}$-$PDPA_{70}$ it appears that all cells within the epithelium contain polymersomes (Fig. 7d) and display high levels of fluorescence. There is no dark region between the upper epithelium and connective tissue component in Fig. 7d, suggesting polymersomes have diffused to the epithelial/connective tissue interface and have been internalized by basal, as well as more superficial, epithelial cells. The TEOM exposed to PEO_{23}-$PDPA_{15}$ expressed high levels of polymersome uptake and fluorescence in the upper layers of the epithelium, but less uptake and fluorescence in the deeper layers of the epithelium compared to $PMPC_{25}$-$PDPA_{70}$ polymersomes (Fig. 7g). The PEO_{23}-$PDPA_{15}$ polymersome diffusion pattern is less uniform and appears patchy. However, this may be due to differences in fluorescence intensity between the two polymersome formulations.

Confocal images were also used to obtain quantitative information about the penetration of the two polymersome formulations into the TEOM. Z_{max} was calculated from the top of the sample to the deepest point of rhodamine fluorescence with higher intensity than the control (Fig. 8a). The depth of penetration was very similar for the two types of polymersome.

DISCUSSION

The aim of this study was to explore the use of TEOM as a convenient surrogate for normal oral mucosa to examine the penetration of two novel forms of polymersomes through oral mucosa using CLSM. These polymersomes are being developed to deliver drugs, proteins or genes into tissues for future clinical use. Information on their penetration into tissues is clearly an important part of their development.

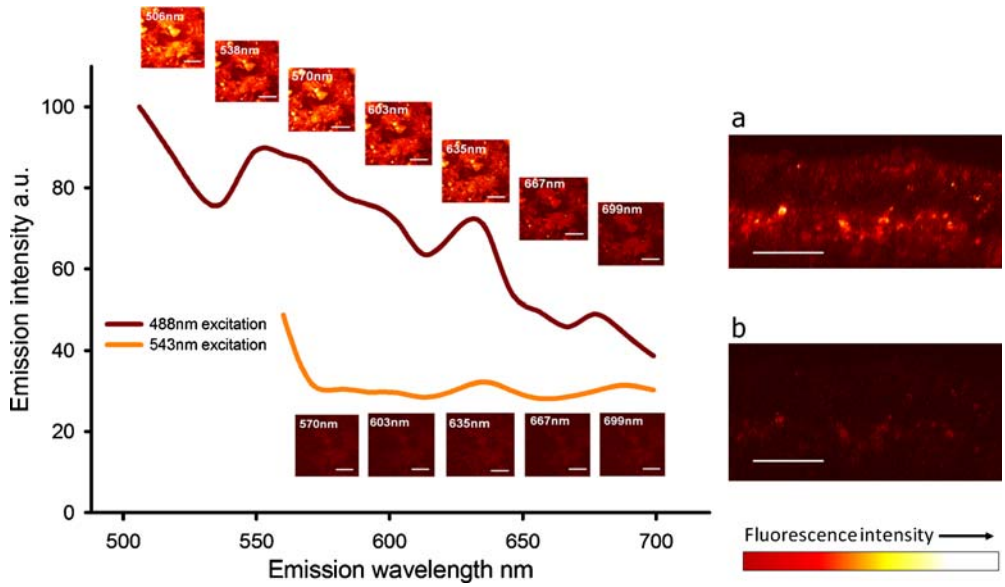

Fig. 4. Emission spectra of TEOM without polymersomes when excited with 488 nm and 543 nm lasers. *z–x* section of TEOM excited at 488 nm (**a**), and at 543 nm (**b**). *Scale bar* 50 μm.

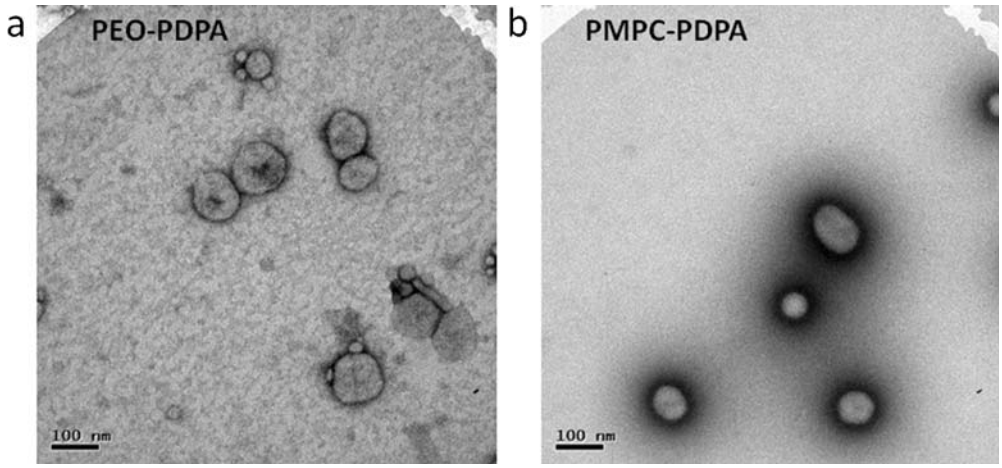

Fig. 5. TEM images of PEO_{23}-$PDPA_{15}$ (**a**) and $PMPC_{25}$-$PDPA_{70}$ (**b**).

This study showed time-dependent penetration of polymersomes into the epithelium of a TEOM model over 48 h. The TEOM used in this study closely resembles normal oral mucosa with epithelial cell differentiation and stratification, minimal keratinization of superficial epithelial layers and a well attached epithelium on a collagenous connective tissue containing fibroblasts (38). MacKenzie *et al.* demonstrated that fibroblasts and subepithelial connective tissue influence the formation of epithelia (40). Factors released by fibroblasts in the connective tissue affect keratinocyte differentiation and proliferation (41). Culturing the model at an air–liquid interface encourages the epithelial cells to differentiate, stratify and organize themselves to imitate natural oral mucosa (Fig. 3).

To successfully image the diffusion of polymersomes through the TEOM, autofluorescence of the TEOM needed to be taken into account. By measuring the fluorescence emission across a range of wavelengths a lambda stack was obtained. This shows the autofluorescence has a broad emission when excited at 488 nm but this is negligible when excited with a 543 nm laser (Fig. 4). Therefore, labelling the polymersomes with rhodamine 6G (maximally excited at 543 nm) allowed us to track their diffusion throughout the model using CLSM. The autofluorescence from 488 nm excitation is useful to judge the spatial location of the polymersomes. Using CLSM we could clearly track the penetration of both $PMPC_{25}$-$PDPA_{70}$ and PEO_{23}-$PDPA_{15}$ rhodamine-labelled polymers over time. The $PMPC_{25}$-$PDPA_{70}$ polymersomes appear to penetrate the epithelium move more quickly and over a more widespread area than the PEO_{23}-$PDPA_{15}$ polymersomes. After 48 h the fluorescence generated by the $PMPC_{25}$-$PDPA_{70}$ polymersomes follows the contours of the basal epithelial cells which reside along the basement membrane, strongly suggesting that these polymersomes diffuse as far as the basement membrane. The PEO_{23}-$PDPA_{15}$ polymersomes did not appear to diffuse as much as the $PMPC_{25}$-$PDPA_{70}$ polymersomes, although spots of fluorescence could still be observed deep within the epithelium with this polymer.

The hydrophobic portion of both polymers is the PDPA block. This component is pH-sensitive; below its pK_a of 6.4 the PDPA block is hydrophilic. When the block copolymer is above its pK_a the PDPA chain becomes hydrophobic, which drives the self-assembly of polymersomes. This hydrophobic block becomes shielded from the aqueous solution by the PMPC or PEO block when in the polymersome configuration. PEO, also known as PEG, is a biocompatible polymer which exhibits very low protein adsorption; it is non-immunogenic and non-antigenic (42). Therefore PEO_{23}-$PDPA_{15}$ polymersomes are unable to bind to cell membrane

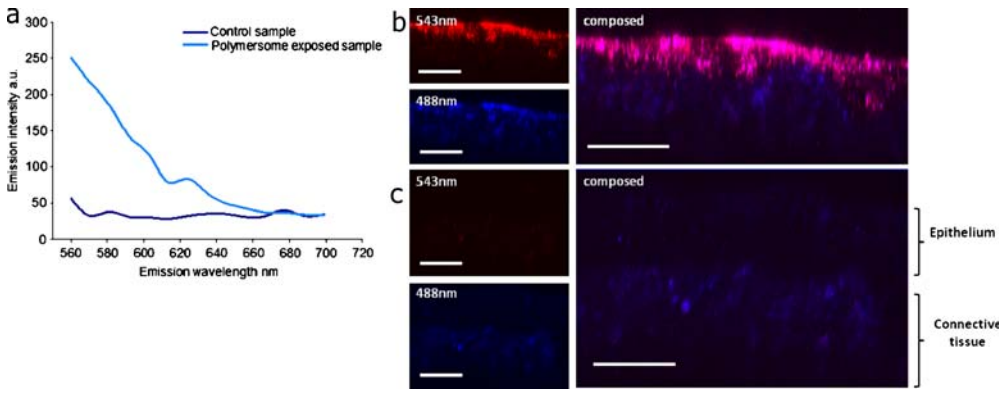

Fig. 6. Emission spectra of tissue engineered oral mucosa after exposure to rhodamine-labelled polymersomes excited at 543 nm (**a**). *z*–*x* section of TEOM exposed to $PMPC_{25}$-$PDPA_{70}$ polymersomes for 48 h (**b**), *z*–*x* section of TEOM with no polymersome exposure (**c**). *Blue*=488 nm excitation. *Red*=543 nm excitation. *Scale bar* 50 μm.

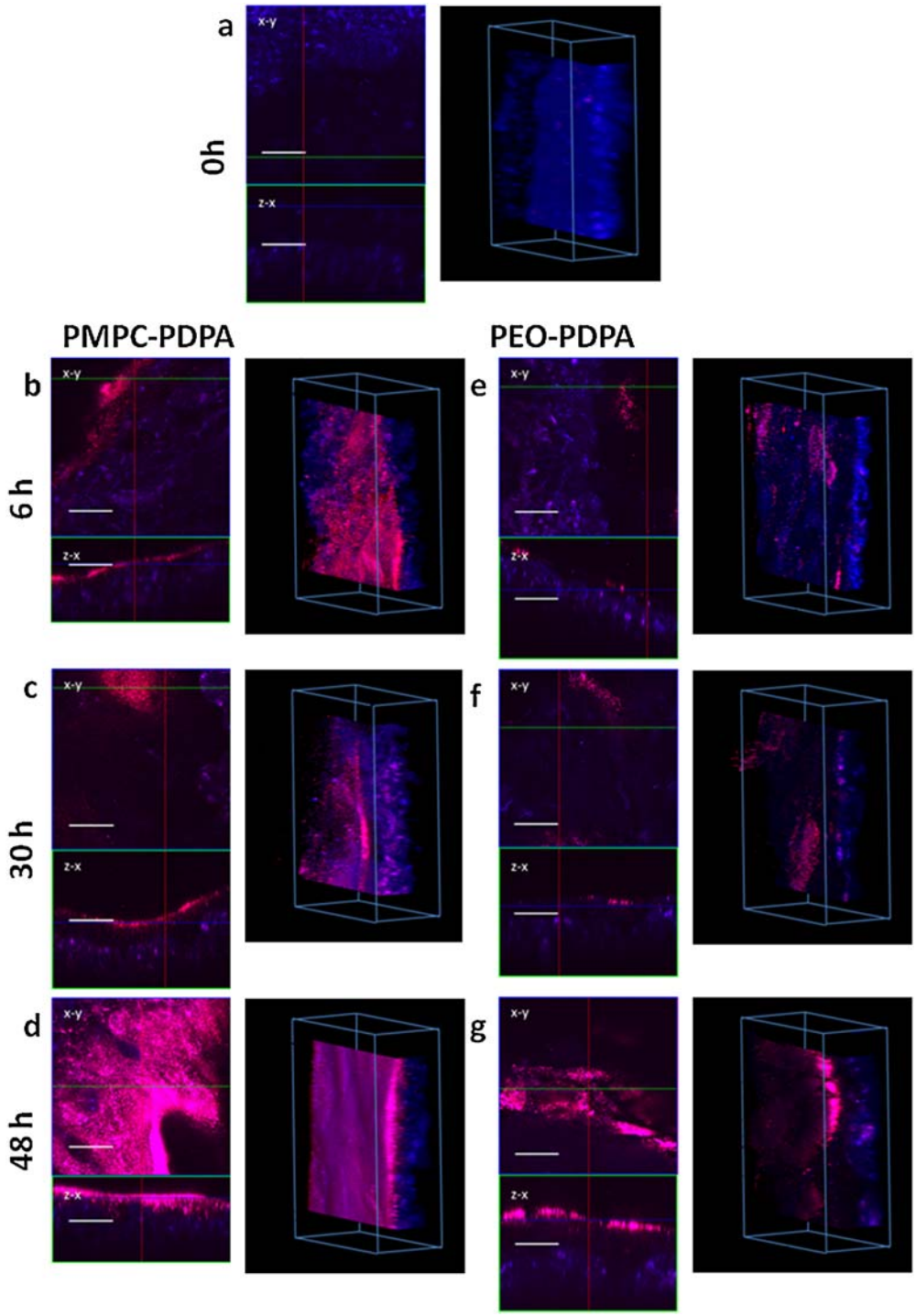

Fig. 7. Tissue engineered models were exposed to rhodamine-labelled $PMPC_{25}$-$PDPA_{70}$ or PEO_{23}-$PDPA_{15}$ polymersomes for 6, 30 or 48 h. (**a**) shows control sample, no exposure to polymersomes. CLSM images of TEOM exposed to $PMPC_{25}$-$PDPA_{70}$ for 6 h (**b**), 30 h (**c**) or 48 h (**d**). TEOM exposed to PEO_{23}-$PDPA_{15}$ polymersomes for 6 h (**e**), 30 h (**f**) or 48 h (**g**). Images on the *left* show *x–y* and *x–z* sections. Images on the *right* are three-dimensional projections of these models, approximately 200μm × 200μm × 100μm. *Scale bar* 50 μm.

proteins, limiting the amount of polymersomes internalized by the cells (43). PMPC is also non-fouling to proteins when expressed at a surface. However, $PMPC_{25}$-$PDPA_{70}$ polymersomes bind more strongly to cell membranes when compared to PEO_{23}-$PDPA_{15}$ increasing the amount of polymersomes internalized (25,43). The behaviours seen from the two different polymersome preparations may both be clinically useful.

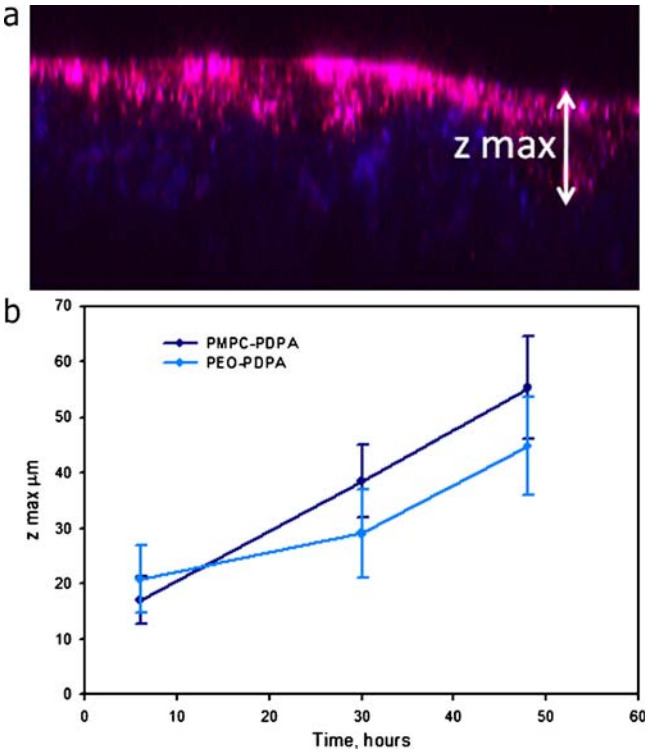

Fig. 8. Depth of penetration (z_{max}) for $PMPC_{25}$-$PDPA_{70}$ polymersomes into the model as measured by analysing the *x–z* and *y–z* projections (**a**). Depth of penetration over time for the two different polymersome formulations (**b**).

The oral epithelium provides a defensive barrier preventing unwanted materials from entering the body and retaining fluid within the mucosa (38). This barrier also prevents many therapeutic agents from crossing the epithelium. For diseases of the oral mucosa such as lichen planus and squamous cell carcinoma, which affect the basal cells of the epithelium, intra-epithelial drug delivery is desirable (34,44). Topical delivery is an important method for delivering drugs at high concentration into diseased oral mucosa whilst limiting any systemic toxicity or side effects. Currently, only a limited range of drugs such as topical steroid preparations can be delivered across the epithelial permeability barrier and into basal epithelial cells. Developing drug delivery systems that can carry a wider array of therapeutic agents across the epithelial permeability barrier, *e.g.* biological agents and genes, and delivering them with high efficiency into basal keratinocytes, would open up a broad spectrum of potentially more effective therapeutic tools for treating many oral mucosal diseases.

For other diseases, widespread systemic delivery of drugs is desirable. For convenience, this is achieved wherever possible by oral administration. Unfortunately, this is not possible with many novel therapeutic agents, particularly biological compounds such as peptides and antibodies (45). If delivered orally, these compounds get degraded by enzymes within the digestive system. As a result, such drugs often have to be given parenterally *i.e.* by injection. This severely limits the usefulness of these drugs, particularly for the treatment of chronic and less severe diseases where they would otherwise revolutionize treatment. Trans-epithelial delivery offers the prospect of a more practical and effective method of delivering such drugs if the permeability barrier can be overcome without damaging the therapeutic agent or disrupting the epithelium (35,46). For trans-epithelial delivery, a vector that crosses the epithelium and is not retained by epithelial cells but delivers its contents into the connective tissue or circulation is highly desirable. Current examples of effective trans-epithelial drug delivery in the oral mucosa include the delivery of Diazepam to treat patients with status epilepticus and the delivery of glyceryl trinitrate for the relief of episodes of angina (35).

The permeability barrier of TEOM is very similar to that of normal human oral mucosa (6). This permeability barrier is due to the supra-basal cells (Fig. 3), also known as spinous cells. These cells begin to differentiate from the stem cell-like basal cells as they move towards the surface of the epithelia where they form strong intercellular desmosomal junctions and release sphingolipids into the surrounding intercellular spaces to produce a barrier which is impermeable to water soluble molecules (47).

There are two methods of diffusion across the epithelial permeability barrier. From the current data we are unable to determine which path is taken by our polymersomes. However, there are two possible routes: (1) the intercellular pathway where material passes through lipid-rich domains around the cells and (2) the trans-cellular pathway where material passes in and out of the cells in each layer (34). Tight junctions which are, found in the superficial layer of the epithelia, force material to pass through the cells. These junctions are not sufficiently widespread enough in the oral epithelium to completely prevent material using the intercellular pathway but are more widespread in the skin (47). The polymersome membranes are highly deformable, enabling them to pass through gaps between cells in tissues such as the oral epithelium that are smaller than their own diameter. The deformability of polymersomes has been demonstrated (12) using micropipette aspiration of giant (20–50 μm) polymersomes. The diffusion of polymersomes across the oral epithelium may not be driven by a concentration gradient but rather via a hydration gradient across the different layers (48). In the epithelium the hydration gradient pulls the carriers through the relatively dehydrated keratinized layer until they reach the viable epithelium, where there is a higher level of hydration. These rather bulky carriers may then be pushed through the lower layers of the epithelium by more carriers, which are drawn into the epithelium by the hydration gradient (48).

Both polymersome formulations are able to penetrate into the oral epithelium, demonstrating they can travel across the permeability barrier of our TEOM. Further research is needed to determine by which mechanism these polymersomes pass across the epithelium. However, the method of tracking the polymersomes described in this paper is an important first step.

CONCLUSION

The TEOM model combined with CLSM is an effective and versatile model to monitor the diffusion and penetration of polymersomes into oral mucosa. Confocal microscopy can be used to both image the diffusion and to quantify the depth of penetration. $PMPC_{25}$-$PDPA_{70}$ and PEO_{23}-$PDPA_{15}$ polymersomes are both able to diffuse through the tissue

engineered epithelia in a time-dependent manner. The depth of penetration of the two polymers is very similar. Both formulations may have clinical potential for the intra- and/or trans-epithelial delivery of therapeutic agents.

ACKNOWLEDGMENTS

We would like to thank Dr. Anthony Bullock, Dr. Helen Colley, Mr. Tom Smart and Ms. Marzia Massignani for their help and guidance. This work was supported by funding from EPSRC (DTA PhD studentship to Vanessa Hearnden) and Biocompatibles UK Ltd.

REFERENCES

1. MacNeil S. Progress and opportunities for tissue-engineered skin. Nature 2007;445:874–80. doi:10.1038/nature05664.
2. Moharamzadeh K, Brook IM, Van Noort R, Scutt AM, Thornhill MH. Tissue-engineered oral mucosa: a review of the scientific literature. J Dent Res. 2007;86:115–24. doi:10.1177/154405910708600203.
3. Schmalz G. Materials science: biological aspects. J Dent Res. 2002;81:660–3. doi:10.1177/154405910208101001.
4. Schmalz G, Schuster U, Koch A, Scheweikl H. Cytotoxicity of low pH dentin-bonding agents in a dentin barrier test *in vitro*. J Endod. 2002;28:188–92. doi:10.1097/00004770-200203000-00011.
5. Chakrabarty KH, Dawson RA, Harris P, Layton C, Babu M, Gould L, Phillips J, Leigh I, Green C, Freedlander E, Mac Neil S. Development of autologous human dermal–epidermal composites based on sterilized human allodermis for clinical use. Br J Dermatol. 1999;141:811–23. doi:10.1046/j.1365-2133.1999.03153.x.
6. Selvaratnam L, Cruchley AT, Navsaria H, Wertz PW, Hagi-Pavli EP, Leigh IM, Squier CA, Williams DM. Permeability barrier properties of oral keratinocyte cultures: a model of intact human oral mucosa. Oral Dis. 2001;7:252–8. doi:10.1034/j.1601-0825.2001.70409.x.
7. Bhargava S, Chapple CR, Bullock AJ, Layton C, MacNeil S. Tissue-engineered buccal mucosa for substitution urethroplasty. BJU Int. 2004;93:807–11. doi:10.1111/j.1464-410X.2003.04723.x.
8. Bhargava S, Patterson JM, Inman RD, MacNeil S, Chapple CR. Tissue-engineered buccal mucosa urethroplasty—clinical outcomes. Eur Urol. 2008;53:1263–71. doi:10.1016/j.eururo.2008.01.061.
9. Smart T, Lomas H, Massignani M, Flores-Merino MV, Perez LR, Battaglia G. Block copolymer nanostructures. Nanotoday 2008;3:1–9.
10. Du J, Tang Y, Lewis AL, Armes SP. pH-sensitive vesicles based on a biocompatible zwitterionic diblock copolymer. J Am Chem Soc. 2005;127:17982–3. doi:10.1021/ja056514l.
11. Madsen J. PhD thesis, University of Sheffield; 2009
12. Discher BM, Won Y, Ege DS, Lee JCM, Bates FS, Discher DE, Hammer DA. Polymersomes: tough vesicles made from diblock copolymers. Science 1999;284:1143–6. doi:10.1126/science.284.5417.1143.
13. Discher DE, Eisenberg A. Polymer vesicles. Science 2002;297:967–73. doi:10.1126/science.1074972.
14. Bangham AD. A correlation between surface charge and coagulant action of phospholipids. Nature 1961;192:1197–8. doi:10.1038/1921197a0.
15. Lasic DD, Papahadjopoulos D. Medical applications of liposomes. Amsterdam: Elsevier; 1998.
16. Photos PJ, Bacakova L, Discher B, Bates FS, Discher DE. Polymer vesicles *in vivo*: correlations with PEG molecular weight. J Control Release 2003;90:323–34. doi:10.1016/S0168-3659(03)00201-3.
17. Lasic DD. Sterically stabilized vesicles. Angew Chem Int Ed. 1994;33:1685–98. doi:10.1002/anie.199416851.
18. Lasic DD. Recent developments in medical applications of liposomes: sterically stabilized liposomes in cancer therapy and gene delivery *in vivo*. J Control Release 1997;48:203–22. doi:10.1016/S0168-3659(97)00045-X.
19. Duncan R. The dawning era of polymer therapeutics. Nat Rev Drug Discov. 2003;2:347–60. doi:10.1038/nrd1088.
20. Discher DE, Ortiz V, Srinivas G, Klein ML, Kim Y, Christian D, Cai S, Photos P, Ahmed F. Emerging applications of polymersomes in delivery: from molecular dynamics to shrinkage of tumors. Prog Polym Sci. 2007;32:838–57. doi:10.1016/j.progpolymsci.2007.05.011.
21. Battaglia G, Ryan A. Bilayers and interdigitation in block copolymer vesicles. J Am Chem Soc. 2005;127:8757–64. doi:10.1021/ja050742y.
22. Battaglia G, Ryan AJ, Tomas S. Polymeric vesicle permeability: a facile chemical assay. Langmuir 2006;22:4910–3. doi:10.1021/la060354p.
23. Aranda-Espinoza H, Bermudez H, Bates FS, Discher DE. Electromechanical limits of polymersomes. Phys Rev Lett. 2001;87:208301. doi:10.1103/PhysRevLett.87.208301.
24. Lomas H, Canton I, MacNeil S, Du J, Armes SPA, Ryan AJ, Lewis AL, Battaglia G. Biomimetic pH sensitive polymersomes for efficient DNA encapsulation and delivery. Adv Mater. 2007;19:4238–43. doi:10.1002/adma.200700941.
25. Lomas H, Massignani M, Abdullah KA, Canton I, Lo Presti C, MacNeil S, Du J, Blanazs A, Madsen J, Armes SP, Lewis AL, Battaglia G. Non-cytotoxic polymer vesicles for rapid and efficient intracellular delivery. Faraday Discuss 2008;139:143. doi:10.1039/b717431d.
26. Rameez S, Alosta H, Palmer AF. Biocompatible and biodegradable polymersome encapsulated hemoglobin: a potential oxygen carrier. Bioconjugate Chem. 2008;19:1025–32. doi:10.1021/bc700465v.
27. Arifin DR, Palmer AF. Polymersome encapsulated hemoglobin: a novel type of oxygen carrier. Biomacromolecules 2005;6:2172–81. doi:10.1021/bm0501454.
28. Ghoroghchian PP, Frail PR, Susumu K, Blessington D, Brannan AK, Bates FS, Chance B, Hammer DA, Therien MJ. Near-infrared-emissive polymersomes: self-assembled soft matter for *in vivo* optical imaging. PNAS 2005;102:2922–7. doi:10.1073/pnas.0409394102.
29. Lin JJ, Ghoroghchian PP, Zhang Y, Hammer DA. Adhesion of antibody-functionalized polymersomes. Langmuir 2006;22:3975–9. doi:10.1021/la052445c.
30. Matyjaszewski K, Spanswick J. Controlled/living radical polymerization. Mater Today 2005;8:26–33. doi:10.1016/S1369-7021(05)00745-5.
31. Cerritelli S, Velluto D, Hubbell JA. PEG-SS-PPS: reduction-sensitive disulfide block copolymer vesicles for intracellular drug delivery. Biomacromolecules 2007;8:1966–72. doi:10.1021/bm070085x.
32. Meng F, Engbers GHM, Feijen J. Biodegradable polymersomes as a basis for artificial cells: encapsulation, release and targeting. J Control Release 2005;101:187–98. doi:10.1016/j.jconrel.2004.09.026.
33. Ben-Haim N, Broz P, Marsch S, Meier W, Hunziker P. Cell-specific integration of artificial organelles based on functionalized polymer vesicles. Nano Letters 2008;8:1368–73. doi:10.1021/nl080105g.
34. Sood S, Shiff SJ, Yang CS, Chen X. Selection of topically applied non-steroidal anti-inflammatory drugs for oral cancer chemoprevention. Oral Oncol. 2005;41:562–7. doi:10.1016/j.oraloncology.2005.01.003.
35. Zhang H, Zhang J, Streisand JB. Oral mucosal drug delivery: clinical pharmacokinetics and therapeutic applications. Clin Pharmacokinet. 2002;41:661–80. doi:10.2165/00003088-200241090-00003.
36. Robinson KL, Weaver JVM, Armes SP, Diaz Marti E, Meldrum F. Synthesis of controlled-structure sulfate-based copolymers via atom transfer radical polymerisation and their use as crystal habit modifiers for $BaSO_4$. J Mater Chem. 2002;12:890–6. doi:10.1039/b200348c.
37. Rheinwald JG, Green H. Serial cultivation of strains of human epidermal keratinocytes: the formation of keratinizing colonies from single cells. Cell 1975;6:331–43. doi:10.1016/S0092-8674(75)80001-8.
38. Nanci A. Ten Cate's oral histology—development, structure and function. St. Louis: Mosby; 2003.
39. Schenke-Layland K, Riemann I, Damour O, Stock UA, König K. Two-photon microscopes and *in vivo* multiphoton tomographs—

powerful diagnostic tools for tissue engineering and drug delivery. Adv Drug Deliv Rev. 2006;58:878–96. doi:10.1016/j.addr.2006.07.004.
40. Mackenzie IC, Fusenig NE. Regeneration of organized epithelial structure. J Invest Dermatol. 1983;81:189s–94s. doi:10.1111/1523-1747.ep12541093.
41. Costea DE, Loro LL, Dimba EAO, Vintermyr OK, Johannessen AC. Crucial effects of fibroblasts and keratinocyte growth factor on morphogenesis of reconstituted human oral epithelium. J Invest Dermatol. 2003;121:1479–86. doi:10.1111/j.1523-1747.2003.12616.x.
42. Alcantar NA, Aydil ES, Israelachvili JN. Polyethylene glycol-coated biocompatible surfaces. J Biomed Mater Res. 2000;51:343–51. doi:10.1002/1097-4636(20000905)51:3<343::AID-JBM7>3.0.CO;2-D.
43. Massignani M, Blanazs A, Madsen J, Armes SP, Lewis AL, Battaglia G. Engineering polymeric nanovectors for effective and rapid cellular delivery. In preparation (2008).
44. Campisi G, Giandalia G, De Caro V, Di Liberto C, Aricò P, Giannola LI. A new delivery system of clobetasol-17-propionate (lipid-loaded microspheres) compared with a conventional formulation (lipophilic ointment in a hydrophilic phase) in topical treatment of atrophic/erosive oral lichen planus. A Phase IV, randomized, observer-blinded, parallel group clinical trial. Br J Dermatol. 2004;150:984–90. doi:10.1111/j.1365-2133.2004.05943.x.
45. Blanchette J, Kavimandan N, Peppas NA. Principles of transmucosal delivery of therapeutic agents. Biomed Pharmacother. 2004;58:142–51. doi:10.1016/j.biopha.2004.01.006.
46. Guy RH. Current status and future prospects of transdermal drug delivery. Pharm Res. 1996;13:1765–9. doi:10.1023/A:1016060403438.
47. Shimono M, Clementi F. Intercellular junctions of oral epithelium. I. Studies with freeze-fracture and tracing methods of normal rat keratinized oral epithelium. J Ultrastruct Res. 1976;56:121–36. doi:10.1016/S0022-5320(76)80145-1.
48. Cevc G, Gebauer D. Hydration-driven transport of deformable lipid vesicles through fine pores and the skin barrier. Biophys J. 2003;84:1010–24. doi:10.1016/S0006-3495(03)74917-0.